Journal of Power Sources 244 (2013) 35–42

Contents lists available at SciVerse ScienceDirect

Journal of Power Sources

journal homepage: www.elsevier.com/locate/jpowsour

Preparation and characterization of spinel $LiNi_{0.5-x}Mg_xMn_{1.5}O_4$ cathode materials via spray pyrolysis method

Je-Jang Shiu, Wei Kong Pang, She-huang Wu*

Department of Materials Engineering, Tatung University, Taipei 104, Taiwan, ROC

HIGHLIGHTS

- Establishment of structure–function relationship of $LiNi_{0.5}Mn_{1.5}O_4$ cathode material for lithium ion battery.
- Combination of neutron powder diffraction and X-ray diffraction studies on the structure and crystallographic analysis.
- Substitution effects of Mg on the electrochemical properties of $LiNi_{0.5}Mn_{1.5}O_4$.
- Discussion on electrochemical dissimilarities on $P4_332$ and $Fd\bar{3}m$ phases.

ARTICLE INFO

Article history:
Received 12 November 2012
Received in revised form
15 April 2013
Accepted 16 April 2013
Available online 23 April 2013

Keywords:
High-voltage spinel material
Spray pyrolysis
Magnesium-substitution
Lithium ion batteries

ABSTRACT

Mg-substituted $LiNi_{0.5-x}Mg_xMn_{1.5}O_4$ (x = 0, 0.02, 0.05, and 0.10) are prepared via a spray pyrolysis method followed by a two-step heating at 600 °C for 6 h and 800 °C for 8 h in air. The compositions, morphology, and crystalline structure are studied with ICP-OES, SEM, XRD, and NPD, respectively. The XRD and NPD results are refined with Rietveld method to reveal the crystallography and phase composition of the prepared samples. The electrochemical properties of the obtained samples are investigated with results of capacity retention and cyclic voltammetric studies. Samples synthesized in this study manifest promising rate capability that may be due to the presence of major $Fd\bar{3}m$ phase with a minor amount of $P4_332$. Among the prepared samples, $LiNi_{0.4}Mg_{0.1}Mn_{1.5}O_4$ demonstrates the lowest capacity fading rate among the prepared samples at 0.1 ~ 5C rates when cycled between 3.5 and 5.1 V at temperatures of 30 and 60 °C.

1. Introduction

$LiMn_2O_4$ has been considered as one of the most promising cathode materials due to its non-toxicity, low cost, high thermal stability, and good electrochemical properties [1,2]. However, rapid loss of capacity upon cycling especially at elevated temperatures and low theoretical capacity limit its commercial applications. Various methods have been developed to improve the cycling performance of $LiMn_2O_4$ materials, such as doping with cations and anions [3–8], surface coating with oxides and nano particles [9,10], and adding electrolyte additives [11,12]. It has been found that $LiMn_2O_4$-based materials with Co, Ni, or Cr doping can significantly lower the capacity loss at 4 V plateau though the capacity is also lowered by the increasing doping level of electrochemically-inert ions when cycling between 3.0 and 4.3 V [6–8]. In addition to the ordinary 4 V plateau, new plateaus, ascribing to the redox couple of Co^{2+}/Co^{4+}, Ni^{2+}/Ni^{4+}, and Cr^{3+}/Cr^{4+}, at voltage higher than 4.5 V were also reported when doping level higher than 5% and cycled up to voltages higher than 4.8 V [13–18]. Yoon et al. prepared $LiM_{0.5}Mn_{1.5}O_4$ (M = Co, Cr, and Ni) via a solid-state method by calcination at 1000 °C for 24 h in oxygen atmosphere followed by heating at 700 °C for 30 h to stabilized spinel-like crystalline structure [15]. The valences of Co, Cr, and Ni determined from XPS are 2+, 3+, and 2+, respectively. From the discharge profiles of the prepared $LiM_{0.5}Mn_{1.5}O_4$ in voltage range between 3.5 and 5.2 V at a current density of 0.65 mA cm^{-2}, a 4.7 V plateau due to reduction of M^{4+} and a 4 V plateau due to Mn^{4+}/Mn^{3+} are observed. For Co and Ni-substituted samples, 4.7 V plateau is significantly longer than the 4 V plateau, whereas 4 V and 4.7 V plateaus with commensurate length are found in Cr-substituted sample. Similar results are also reported by Ohzuku et al., except the capacity of Co-substituted sample is significantly contributed equally by both 4 V and 5 V plateaus [18]. From the results reported previously [13–18], $LiNi_{0.5}Mn_{1.5}O_4$ has been suggested as a promising cathode material for lithium ion battery due to its high energy density that

* Corresponding author. Tel.: +886 2 25922458; fax: +886 2 25936897.
E-mail address: shwu@ttu.edu.tw (S.-h. Wu).

0378-7753/$ – see front matter © 2013 Elsevier B.V. All rights reserved.
http://dx.doi.org/10.1016/j.jpowsour.2013.04.083

Table 1
Compositions of 800 °C prepared $LiNi_{0.5-x}Mg_xMn_{1.5}O_4$ ($x = 0, 0.02, 0.05, 0.1$) powders determined by ICP-OES.

Sample	Atomic ratios			
	Li	Ni	Mn	Mg
$LiNi_{0.5}Mn_{1.5}O_4$	1.02	0.50	1.50	NIL
$LiNi_{0.48}Mg_{0.02}Mn_{1.5}O_4$	1.02	0.48	1.50	0.02
$LiNi_{0.45}Mg_{0.05}Mn_{1.5}O_4$	1.01	0.45	1.50	0.05
$LiNi_{0.40}Mg_{0.10}Mn_{1.5}O_4$	1.00	0.40	1.50	0.10

Table 2
Lattice parameter of 800 °C prepared $LiNi_{0.5-x}Mg_xMn_{1.5}O_4$ ($x = 0, 0.02, 0.05, 0.1$) powders determined using Rietveld refinements.

Sample	Lattice parameter (Å)
$LiNi_{0.5}Mn_{1.5}O_4$	8.1722(1)
$LiNi_{0.48}Mg_{0.02}Mn_{1.5}O_4$	8.1756(1)
$LiNi_{0.45}Mg_{0.05}Mn_{1.5}O_4$	8.1776(1)
$LiNi_{0.40}Mg_{0.10}Mn_{1.5}O_4$	8.1804(1)

contributed mainly from 4.7 V plateau, excellent cycling performance, and good Coulombic efficiency in the voltage window between 3 and 5.2 V.

$LiNi_{0.5}Mn_{1.5}O_4$ was initially introduced as a 3 and 4 V cathode material, manifesting discharge capacity of ~160 mAh g^{-1} at 3 V when cycling between 2 and 4.2 V by Amine et al. [3]. They also reported that this material shows initial discharge capacity higher than 90 mAh g^{-1} at 4.7 V plateau, which corresponds to the reduction of Ni^{4+} to Ni^{2+}, when cycling between 4.2 and 5.1 V [4]. Thereafter, reversible capacity higher than 100 mAh g^{-1}, attributed to the Ni^{2+}/Ni^{4+} redox reaction at 4.7 V when cell was cycled between 3 and 4.9 V, was also reported by Zhong et al. [14]. This higher working voltage implies that higher energy density can be obtained. Compared with other cathode materials, such as $LiCoO_2$ (~620 Wh kg^{-1}) and $LiFePO_4$ (~591 Wh kg^{-1}), $LiNi_{0.5}Mn_{1.5}O_4$ exhibits high energy density (658 Wh kg^{-1}) because of its high working voltage plateau (4.7 V) and theoretical capacity (146 mAh g^{-1}) [19].

$LiNi_{0.5}Mn_{1.5}O_4$ can crystallize into two different crystallographic structures, cation-ordered $P4_332$ and cation-disordered $Fd\bar{3}m$, depending on the conditions of heat-treatment [20–23]. The ordered–disordered transition has been recommended as a result of oxygen loss from ordered spinel at temperatures higher than 650 °C [22,24], which induces the presence of Mn^{3+} to perturb the Ni^{2+}/Mn^{4+} ordering [24]. Experiments showed that the disordered–ordered transition can also be achieved by post-annealing at temperatures lower than 700 °C in oxygen atmosphere [22,25]. The effects of cation ordering on the cycling performance of $LiNi_{0.5}Mn_{1.5}O_4$ between voltages of 3.5 and 5 V remain controversial. Though it has been showed that the disordered spinels have better cycling performance because of their higher electronic and Li^+-ion conductivities than those of ordered spinels [21,26], ordered spinel obtained by post-annealing under high-pressure oxygen atmosphere at temperature lower than 600 °C did not only manifest higher framework stability than disordered samples, but also exhibited higher capacity and capacity retention than samples quenched from temperatures between 743 and 855 °C [22].

Kunduraci et al. suggested that the rate capability of $LiNi_xMn_{2-x}O_4$ spinels can be positively affected by the presence of Mn^{3+} [24]. However, the existence of Mn^{3+} in $LiNi_{0.5}Mn_{1.5}O_4$ may induce Jahn–Teller distortions and capacity loss upon cycling. The unwanted impurity of $Li_yNi_{1-y}O$ phase can be observed commonly in both $P4_332$ and $Fd\bar{3}m$ samples [24,27,28]. Though the effect of $Li_yNi_{1-y}O$ phase on overall conduction remains unclear, it does lower the specific capacity of spinel $LiNi_{0.5}Mn_{1.5}O_4$. Moreover, the possible decompositions of electrolyte at high operating voltages resulting in the formation of solid electrolyte interface (SEI) layer and the dissolution of active materials at high working temperatures inducing capacity fading hinder the applications of $LiNi_{0.5}Mn_{1.5}O_4$ cathode material in lithium ion batteries [29,30]. To reduce the effects of these shortcomings, several methods, such as metal ion doping [27,31–36], surface modification [30,37,38], and heat treatment conditions optimization [21,24,39,40], have been introduced.

In this study, Mg-substitution was employed to prepare $LiNi_{0.5-x}Mg_xMn_{1.5}O_4$ ($x = 0$, 0.02, 0.05, and 0.10) samples via spray pyrolysis method. The effects of Mg-substitution on the electrochemical performance of $LiNi_{0.5}Mn_{1.5}O_4$ cathodes are discussed with aids of cyclic voltammetric, capacity retention, and electrochemical impedance spectroscopic studies. The crystallographic study on pristine and Mg-substituted $LiNi_{0.5}Mn_{1.5}O_4$ samples was

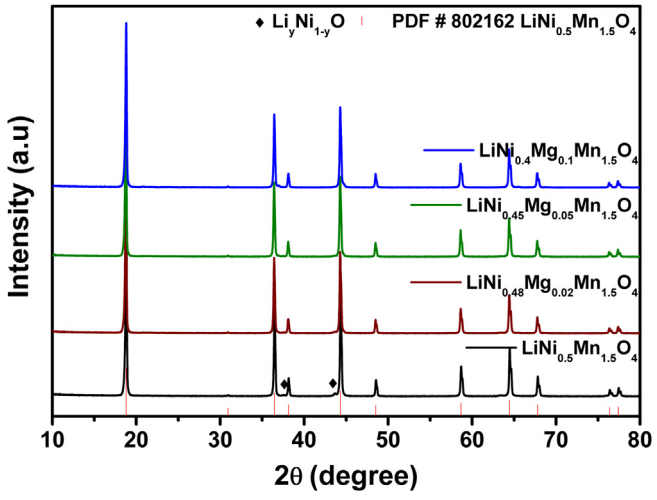

Fig. 1. XRD patterns of $LiNi_{0.5-x}Mg_xMn_{1.5}O_4$ ($x = 0, 0.02, 0.05, 0.1$) powders prepared at 800 °C.

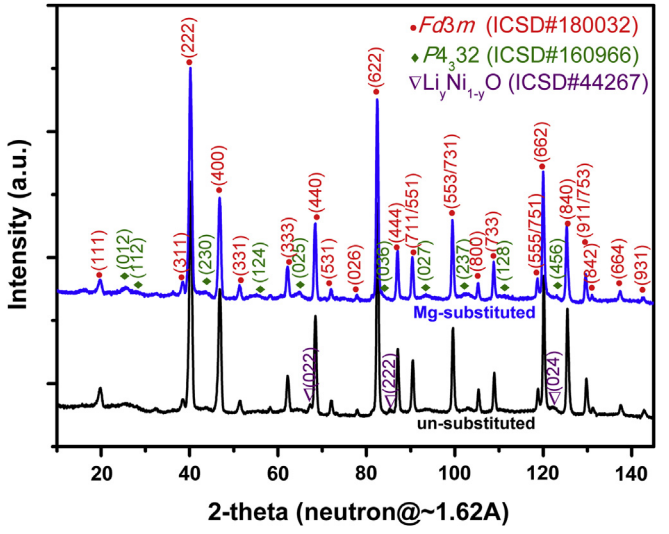

Fig. 2. NPD patterns of $LiNi_{0.5}Mn_{1.5}O_4$ and $LiNi_{0.40}Mg_{0.10}Mn_{1.5}O_4$ powders prepared at 800 °C.

Table 3
Summary of the calculated phase compositions and the corresponding figure-of-merits in Rietveld analysis.

		Un-substituted	Mg-substituted
Phase fraction (mol %)	*Fd*3*m*	79.37 ± 1.22	65.71 ± 1.98
	$P4_332$	17.66 ± 0.63	34.14 ± 1.47
	$Li_yNi_{1-y}O$	2.97 ± 0.18	0.15 ± 0.28
R_{Bragg}	*Fd*3*m*	3.16	4.11
	$P4_332$	2.44	1.96
	$Li_yNi_{1-y}O$	1.73	2.91
Figure-of-merits	R_{wp}	5.91	5.21
	R_{exp}	3.20	4.06
	Goodness-of-fit (χ^2)	3.416	2.099

also performed by Rietveld refinements using X-ray diffraction (XRD) and neutron powder diffraction data (NPD).

2. Experimental

$LiNi_{0.5-x}Mg_xMn_{1.5}O_4$ (x = 0, 0.02, 0.05, 0.1) precursors were prepared via a spray pyrolysis method with citric acid (99.5%, Wako Pure Chem. Ind., Ltd., Japan), $LiNO_3$ (Wako Pure Chem. Ind., Ltd., Japan), $Mn(NO_3)_2{\cdot}6H_2O$ (98.0%, Wako Pure Chem. Ind., Ltd., Japan), $Ni(NO_3)_2{\cdot}6H_2O$ (98.0%, Wako Pure Chem. Ind., Ltd., Japan), and $Mg(NO_3)_2{\cdot}6H_2O$ (98.0%, Wako Pure Chem. Ind., Ltd., Japan) as starting materials. The stoichiometric mixed solutions of the starting materials were mixed thoroughly and then spray dried at temperature of 185 °C. The collected precursors were calcined at 300 °C for 2 h to remove residual organics and the obtained powders were further heat-treated at 600 °C for 6 h and at 800 °C for 8 h in air. The elemental compositions and morphology of the prepared products were investigated by an inductive coupled plasma-optical emission spectrometer (ICP-OES Optima 2100, PerkinElmer Inc., USA) and a scanning electron microscope (JSM-6700F, JEOL Ltd., Japan), respectively. Crystallographic analysis was performed by combining the results obtained from X-ray diffraction (XRD) and neutron powder diffraction (NPD) patterns. XRD data were collected over the range $10° \le 2\theta \le 80°$ on an X-ray diffractometer (XRD6000, Shimadzu Corporation, Japan) using CuKα radiation. The high-resolution NPD data were collected at the Bragg Institute of ANSTO using a high-resolution powder diffractometer (ECHIDNA, Sydney, Australia) with a neutron beam wavelength of ~1.624 Å and a Ge 335 monochromator. The crystalline phase identification and Rietveld refinement were carried out using Rietica ver. 1.7.7 [41]. The optimized parameters used during refinements were background coefficients, zero-shift error, peak shape parameters, and lattice parameters.

The as-synthesized materials were mixed with polyvinylidene fluoride (PVDF, Kynar 741, ELF, Germany) and acetylene black (99.99%, Strem Chemicals Inc., USA) with a weight ratio of 83 : 7 : 10 in adequate amount of *N*-methyl-2-pyrrolidone (NMP, ultra, ISP Technologies Inc., USA) and stirred for 1 day to become slurries. Then the slurries were smeared on an aluminum foil by a doctor blade coater. After drying and pressing, the tapes were punched into 10.0 mm disk electrodes. The prepared electrodes were assembled into CR2032 coin-type cells with Li anodes, 1 M $LiPF_6$ in EC/DMC (volume ratio of 1:1) (Novolyte technologies Co. Ltd., China) electrolyte, and separator (Celgard 2500, Polypore Inc., USA) in an argon-filled glove box. The assembled cells were used for capacity retention studies with a battery tester at 0.1, 1, and 5C rates at 30 and 60 °C. Cyclic voltammetric study was also performed with a potentiostat/galvanostat (Autolab PGSTAT30, Eco Chemie B.V., Netherlands) at a scan rate of 0.1 mV s^{-1} within cutoff voltages of 3.5 and 5.1 V. The electronic conductivity and the charge transfer

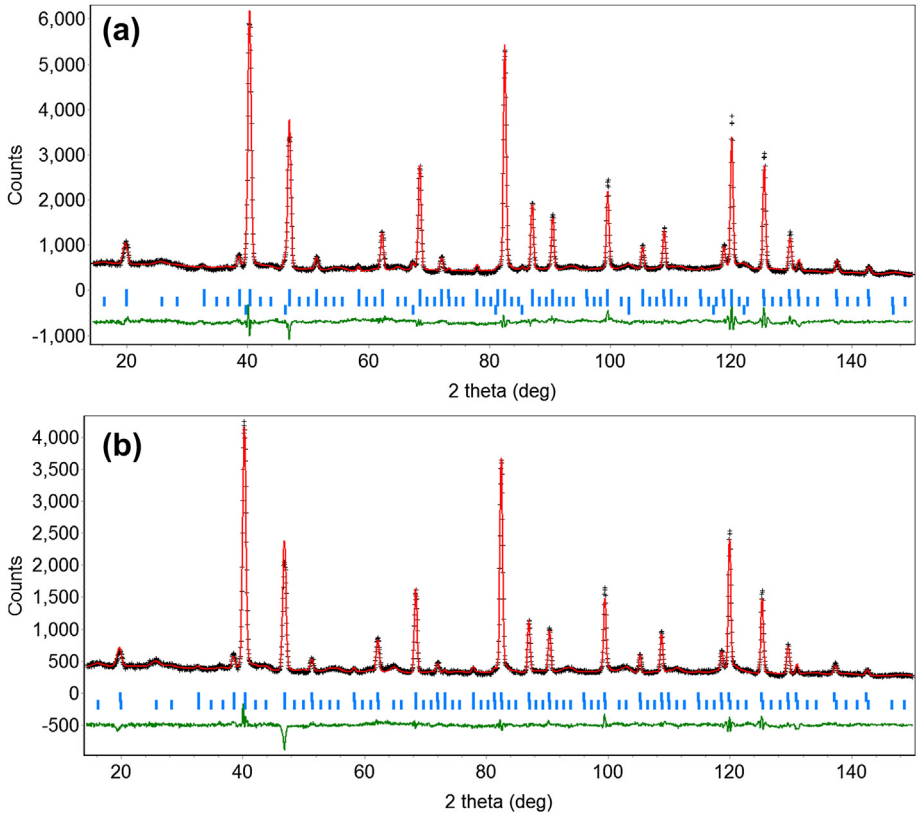

Fig. 3. Rietveld-refined fits for (a) $LiNi_{0.5}Mn_{1.5}O_4$ and (b) $LiNi_{0.4}Mg_{0.1}Mn_{1.5}O_4$ samples using high-resolution NPD data.

resistance of the prepared cathodes were estimated from the results of resistance measurement by four-point probe method with digital multimeter (8845A, Fluke Co., USA) and electrochemical impedance spectroscopic (EIS) study of coin cell prepared with various cathodes with frequency range between 0.1 MHz and 10 mHz on a potentiostat/galvanostat with built-in FRA (VMP3, BioLogic SAS, France).

3. Results and discussion

Elemental compositions of the prepared $LiNi_{0.5-x}Mg_xMn_{1.5}O_4$ ($x = 0$, 0.02, 0.05, and 0.1) powders determined by ICP-OES are listed in Table 1 and these results are close to the expected values. From the XRD patterns, shown in Fig. 1, of the prepared powders, it can be found that pristine $LiNi_{0.5}Mn_{1.5}O_4$ crystallizes in cubic phase with $Fd\bar{3}m$ space group in company with minor amount of $Li_yNi_{1-y}O$ phase. It can also be observed that the amount of $Li_yNi_{1-y}O$ decreases with the substitution level of Mg, showing a good agreement with that reported by Ooms et al. [32], though their samples obtained from ultra-slow cooling process (0.1 °C min^{-1}) were identified as $P4_332$ phase. It may suggest that Mg-substitution has similar effect on suppression of $Li_yNi_{1-y}O$ formation as Ga-substitution [36]. The calculated lattice parameters of $LiNi_{0.5-x}Mg_xMn_{1.5}O_4$ ($x = 0$, 0.02, 0.05, 0.1) samples using XRD data are listed in Table 2. As shown, the lattice parameter increases significantly from 8.1722(1) to 8.1804(1) Å with Mg-substitution level, indicating a lattice expansion caused by the substitution of Mg in $LiNi_{0.5}Mn_{1.5}O_4$ lattice, that is in consistent with those reported previously [32,33]. The values obtained in this study are slightly larger than those reported by Ooms et al., the discrepancy is thought to be originated from the different cooling processes [32]. The thermal-induced expansion can be partially retained in our samples (air-cooling), but it can be totally eliminated in their samples (ultra-slow cooling). Regarding the substitution-induced expansion, it can be simply explained by the larger Mg^{2+} radius

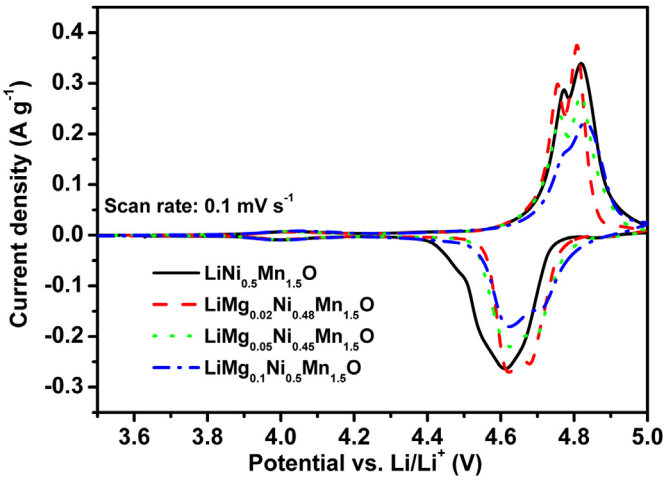

Fig. 5. Cyclic voltammograms of the cells comprised with $LiNi_{0.5-x}Mg_xMn_{1.5}O_4$ ($x = 0$, 0.02, 0.05, and 0.1) cathodes performed with a scan rate of 0.1 mV s^{-1}.

(0.72 Å, coordinate number = 6) than Ni^{2+} (0.69 Å, coordinate number = 6). In order to reveal the detail structure of the prepared powders, high-resolution NPD patterns of pristine and $LiNi_{0.4}Mg_{0.1}Mn_{1.5}O_4$ were collected and refined, as shown in Fig. 2. Though the ordered–disordered transition at about 700 °C have been proposed [20–22,42], coexistence of ordered $P4_332$ (additional reflections at 25.5, 28.2, 64.8°… due to primitive cubic, but not show in face-center cubic) and disordered $Fd\bar{3}m$ (face-center cubic) phases is confirmed in both $LiNi_{0.5}Mn_{1.5}O_4$ and $LiNi_{0.4}Mg_{0.1}Mn_{1.5}O_4$ powders. The phase fractions of the ordered and disorder phases are calculated and tabulated in Table 3. The residual values of the refinement, statistical reliability factor of Bragg (R_B), R-weighted pattern (R_{wp}), $R_{expected}$ (R_{exp}), and the goodness-of-fit (GOF) (χ^2) were also evaluated. It is noted that the

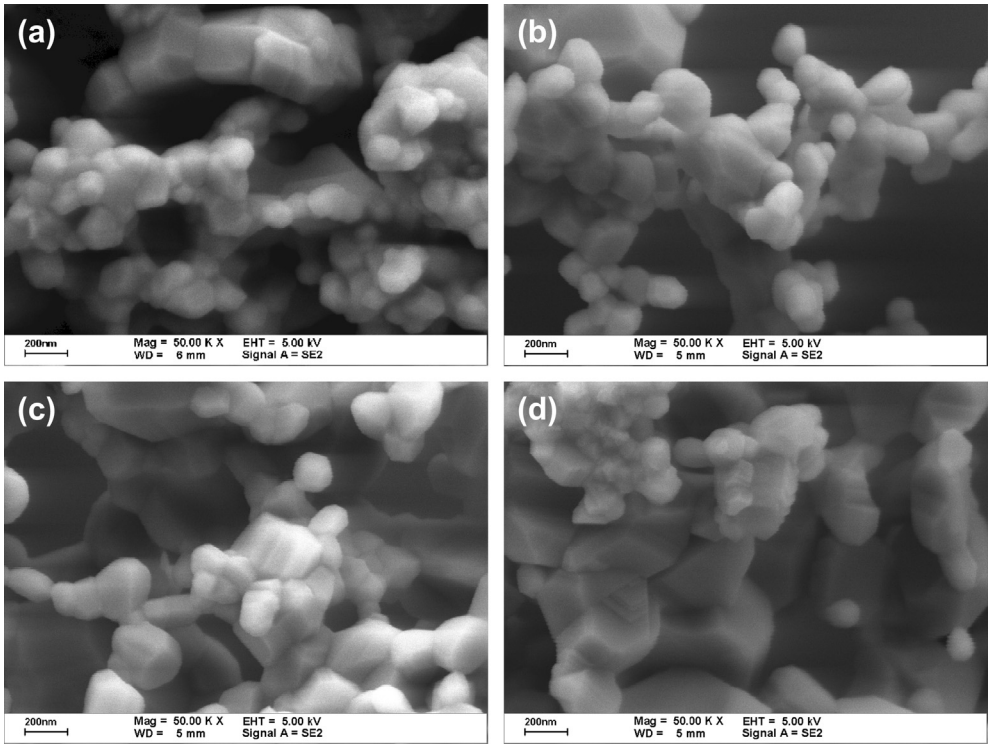

Fig. 4. SEM photographs of the $LiNi_{0.5-x}Mg_xMn_{1.5}O_4$ powders prepared at 800 °C with x = (a) 0, (b) 0.02, (c) 0.05, and (d) 0.1.

χ^2 in Rietica is defined as the square of the ratio of R_{wp} to R_{exp}. The refinement fit profiles are shown in Fig. 3. In contrast, Ooms et al. found the structure of $LiMn_{1.5}Ni_{0.5-\delta}Mg_{\delta}O_4$ ($\delta = 0$, 0.05, and 0.10) powders prepared at 800 °C followed with slow cooling (0.1 °C min^{-1}) are ordered $P4_332$ [32,33]. The discrepancy must be due to different cooling rates after heat-treatments applied. It also can be seen that $LiNi_{0.4}Mg_{0.1}Mn_{1.5}O_4$ contains higher amount of $P4_332$ content than un-substituted sample, implying that Mg-substitution can stabilize the $P4_332$ structure. It is different from the results reported by Shin et al. [36], Ga-substitution can suppress the orderness of spinel structure. For similar ionic radius and same valence of Mg^{2+} (0.72 Å, CN = 6) to Ni^{2+}, the $P4_332$ structure can be retained as Ni^{2+}-like ions (e.g. Mg^{2+}) are substituting. However, when ions having a very different ionic radius (0.62 Å, CN = 6) and valence (3^+) (e.g. Ga^{3+}) are introduced, the disorder structure is preferred.

Fig. 4(a–d) are the SEM micrographs of the 800 °C prepared $LiNi_{0.5-x}Mg_xMn_{1.5}O_4$ ($x = 0$, 0.02, 0.05, and 0.10) powders. The sintering-induced morphologies are clearly observed. The morphologies of the particles are similar and the particle sizes are ranging between 80 and 200 nm for the prepared samples. From this point of view, the particle size effect on the electrochemical properties of the samples can be ruled out and the dissimilarity, in term of performance, of the samples can be considered to be mainly attributed to the Mg-substitution.

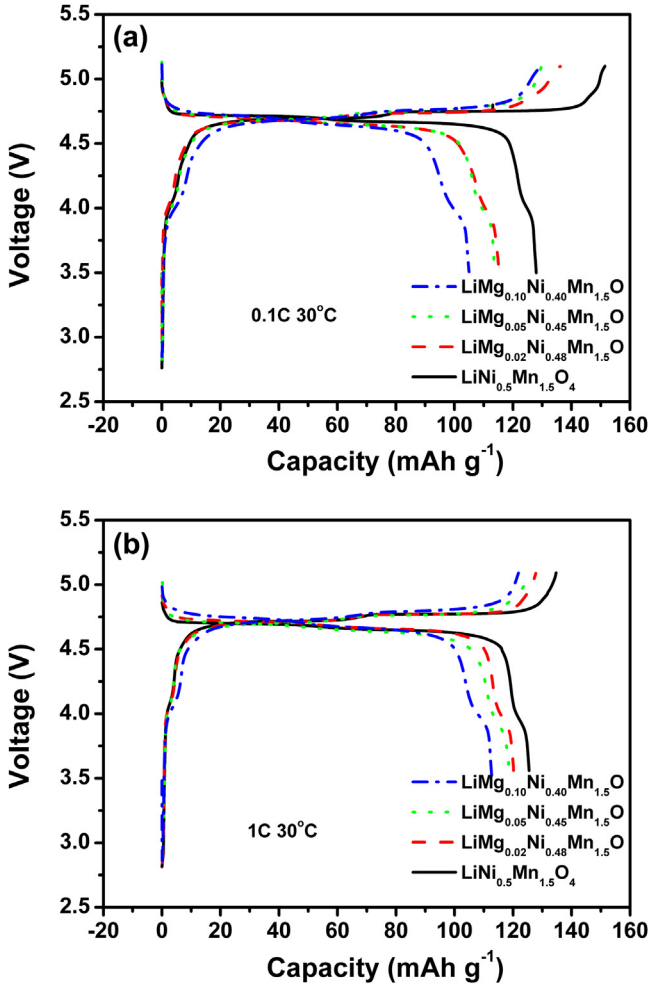

Fig. 6. Charge/discharge curves of the second cycle of cells comprised with $LiNi_{0.5-x}Mg_xMn_{1.5}O_4$ ($x = 0$, 0.02, 0.05, and 0.1) cathodes at (a) 0.1 and (b) 1C rates at 30 °C.

Table 4
Charge/discharge plateau voltages and their differences attributed to the redox reactions for the cells cycled with 0.1C rate at 30 °C.

Samples	Charge/discharge plateau voltages (difference) (V)		
	Mn^{3+}/Mn^{4+}	Ni^{2+}/Ni^{3+}	Ni^{3+}/Ni^{4+}
$LiNi_{0.50}Mn_{1.50}O_4$	4.025/4.001 (0.024)	4.693/4.659 (0.034)	4.748/4.711 (0.037)
$LiNi_{0.48}Mg_{0.02}Mn_{1.50}O_4$	4.014/3.965 (0.049)	4.684/4.641 (0.043)	4.745/4.702 (0.043)
$LiNi_{0.45}Mg_{0.05}Mn_{1.50}O_4$	4.008/3.965 (0.043)	4.688/4.643 (0.045)	4.751/4.706 (0.045)
$LiNi_{0.40}Mg_{0.10}Mn_{1.50}O_4$	4.011/3.961 (0.050)	4.692/4.637 (0.055)	4.763/4.714 (0.049)

The cyclic voltammograms of the cells prepared with $LiNi_{0.5-x}Mg_xMn_{1.5}O_4$ ($x = 0$, 0.02, 0.05, and 0.10) cathodes are plotted in Fig. 5. Anodic/cathodic peaks at around 4.05/3.99, 4.77/4.62, and 4.82/4.69 V vs. Li/Li^+ owing to the redox couples of Mn^{3+}/Mn^{4+}, Ni^{2+}/Ni^{3+}, and Ni^{3+}/Ni^{4+}, are observed, respectively. From the cyclic voltammograms, it can be found that specific capacity (area under curve) may decrease with the increasing of Mg-substitution, whereas the polarization (difference between peak potentials of redox couples) reduces with the Mg-substitution.

Fig. 6 shows the charge/discharge curves of the 2nd cycle of the coin-type cells comprised with 800 °C prepared $LiNi_{0.5-x}Mn_{1.5}Mg_xO_4$ ($x = 0$, 0.02, 0.05, and 0.10) at 0.1 and 1C rates at 30 °C. Plateaus attributed to the Mn^{3+}/Mn^{4+}, Ni^{2+}/Ni^{3+}, and Ni^{3+}/Ni^{4+} can be observed clearly. The charge/discharge plateau voltages of the corresponding redox reactions and their difference at 0.1 and 1C rates are summarized in Tables 4 and 5. The voltage differences are smaller than those determined from cyclic voltammetric study except the difference of Mn^{3+}/Mn^{4+} redox couple. It is owing to the peak currents at Ni^{2+}/Ni^{3+} and Ni^{3+}/Ni^{4+} at cyclic voltammograms are higher than 200 mA g^{-1}, which is higher than 1C, while the peak current at Mn^{3+}/Mn^{4+} is lower than 0.1C rate. Furthermore, the polarization, the voltage differences between the charge/discharge plateaus correspond to each redox reaction, increases slightly with Mg-substitution level, when cells were cycled with 0.1C rate. It is different from the results reported by Ooms et al. [32]. It is noteworthy that ordered $P4_332$ phase was prepared in Ooms et al., whereas mixtures of ordered and disordered phases with majority of $Fd\bar{3}m$ phase were synthesized in this study. Given that diffusivity of Li^+-ions in $P4_332$ structure is lower than that in $Fd\bar{3}m$ phase [21], the increase in voltage difference can be caused by the increasing molar fraction of $P4_332$ phase, induced by Mg-substitution (shown in Table 3). As expected, when cells were cycled with 1C rate, the polarization (voltage differences between charge/discharge plateaus) of each redox reaction is higher than that obtained at 0.1C rate. It can be seen that the rate-induced

Table 5
Charge/discharge plateau voltages and their differences attributed to the redox reactions for the cells cycled with 1C rate at 30 °C.

Samples	Charge/discharge plateau voltages (difference) (V)		
	Mn^{3+}/Mn^{4+}	Ni^{2+}/Ni^{3+}	Ni^{3+}/Ni^{4+}
$LiNi_{0.50}Mn_{1.50}O_4$	4.090/3.945 (0.145)	4.720/4.645 (0.075)	4.774/4.697 (0.077)
$LiNi_{0.48}Mg_{0.02}Mn_{1.50}O_4$	4.014/3.965 (0.111)	4.711/4.655 (0.056)	4.771/4.709 (0.062)
$LiNi_{0.45}Mg_{0.05}Mn_{1.50}O_4$	4.064/3.917 (0.147)	4.702/4.635 (0.067)	4.766/4.702 (0.045)
$LiNi_{0.40}Mg_{0.10}Mn_{1.50}O_4$	4.049/3.974 (0.075)	4.724/4.663 (0.061)	4.796/4.741 (0.055)

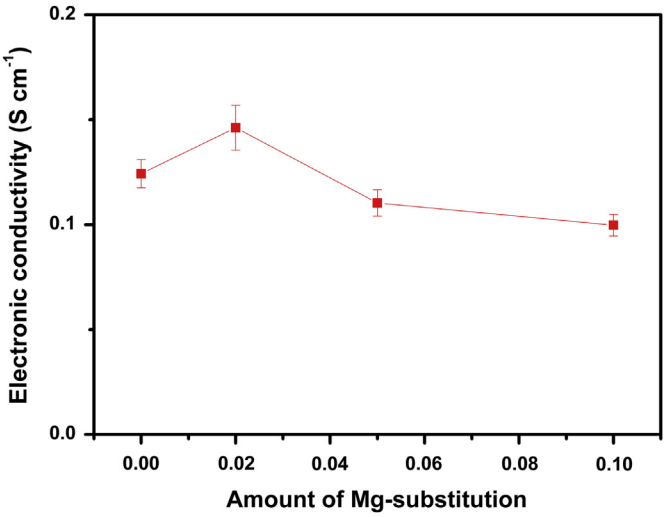

Fig. 7. The plot of electronic conductivity of prepared $LiNi_{0.5-x}Mg_xMn_{1.5}O_4$ ($x = 0$, 0.02, 0.05, and 0.1) cathodes estimated by four-point probe method.

polarization difference is lowered by Mg-substitution. For example, un-substituted $LiNi_{0.5}Mn_{1.5}O_4$ sample exhibits voltage differences of 0.024 V at 0.1C and 0.145 V at 1.0C, whereas $LiNi_{0.4}Mg_{0.1}Mn_{1.5}O_4$ shows 0.050 V at 0.1C and 0.075 V at 1.0C. It can be attributed to the enhancement in electronic conductivity [32], or the decrease in charge transfer resistance by Mg-substitution. In order to investigate the reasons for lowering polarization by Mg-substitution at 1C rate, the electronic conductivity and charge transfer resistance of the prepared $LiNi_{0.5-x}Mn_{1.5}Mg_xO_4$ ($x = 0$, 0.02, 0.05, and 0.10) cathodes are performed and shown in Figs. 7 and 8, respectively. It can be found that the electronic conductivity increases slightly at Mg-substitution level $x = 0.02$, then decreases with amount of Mg-substitution. On the other hand, the results of EIS study reveal that the charge transfer resistance decreases with Mg-substitution. It suggests that the lowering in charge transfer resistance is the cause of the decrease in rate-induced polarization difference with Mg-substitution.

From the charge/discharge curves, the specific charge/discharge capacities decrease because of the reducing amount of Ni^{2+} with increasing amount of Mg-substitution. However, the capacity fading is suppressed significantly by Mg-substitution, shown in Fig. 9. For instances, the average discharge capacity fading rate at 0.1 C decreases from 0.39 to 0.01 mAh g^{-1} per cycle and that of 1C decreases from 0.52 to 0.13 mAh g^{-1} per cycle when Mg-substitution increase to 0.1. It suggests that Mg-substitution can enhance the cycling stability of $LiNi_{0.5}Mn_{1.5}O_4$-based material as reported previously [32,34]. For comparison, the samples prepared in this study show discharge capacities lower at 0.1C, but higher at 1C rate, than those reported by Ooms et al. [32]. That can be attributed to the difference in preparation methods, crystal structures, and phase compositions of the prepared samples. It is confirmed that our samples consist of $Fd\bar{3}m$ major phase with minor $P4_332$ but only $P4_332$ was reported in Ooms's samples, where disordered $Fd\bar{3}m$ phase shows 1 ~ 2 magnitude order higher lithium ion diffusion coefficient (D_{Li}) than the ordered $P4_332$ phase [21].

The results of capacity retention study for the cells comprised with various $LiNi_{0.5}Mn_{1.5}O_4$-based cathodes cycled with 1 and 5C rates at 60 °C are shown in Fig. 10. The cell prepared with pristine $LiNi_{0.5}Mn_{1.5}O_4$ shows similar capacity fading rate (0.52 mAh g^{-1} per cycle) as that cycled at 30 °C with 1C rate, while the cell comprised with $LiNi_{0.4}Mg_{0.1}Mn_{1.5}O_4$ cathode exhibit higher capacity fading rate than those cycled at 30 °C (0.34 at 60 °C to 0.13 mAh g^{-1} per cycle at 30 °C). While the cells are cycled with 5C rate at 60 °C, cells

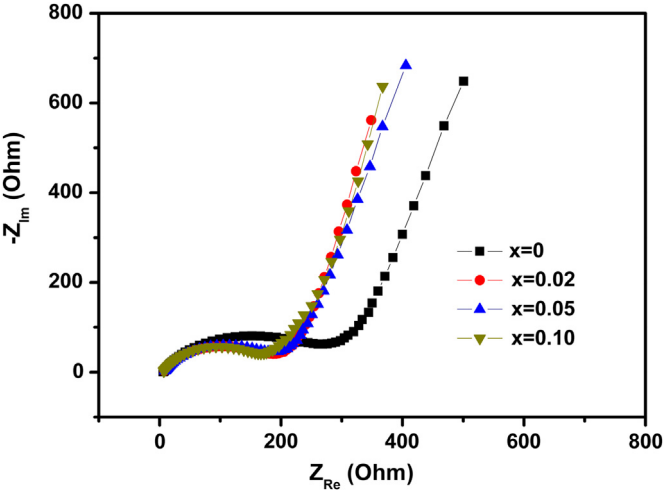

Fig. 8. EIS plots of the prepared $LiNi_{0.5-x}Mg_xMn_{1.5}O_4$/Li cells ($x = 0$, 0.02, 0.05, and 0.1) with frequency range from 0.1 MHz to 10 mHz and amplitude of 5 mV after the cells were initial cycled with 0.1C rate at 30 °C.

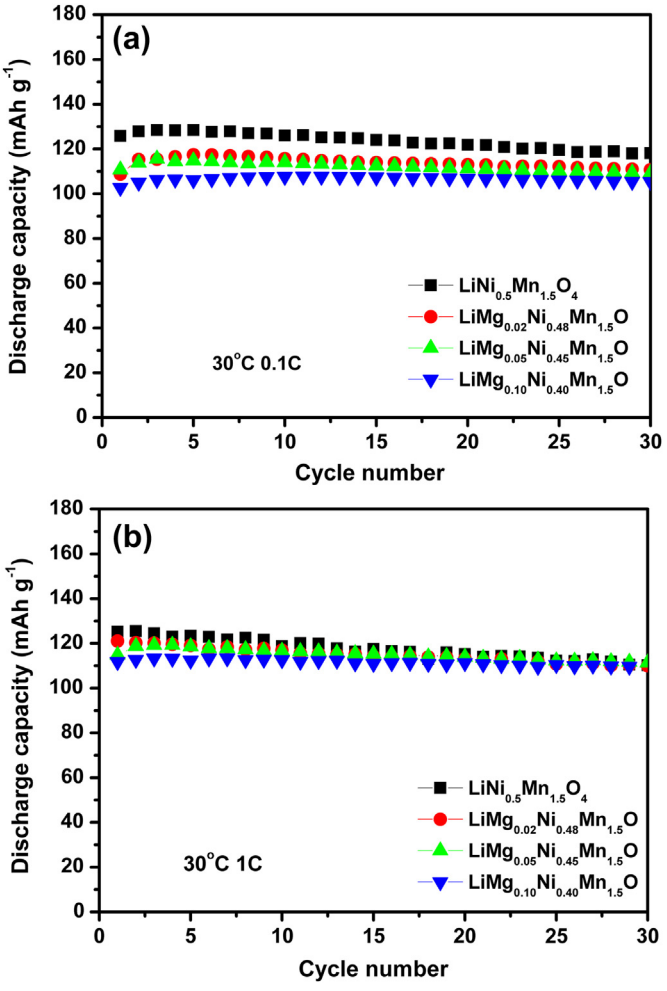

Fig. 9. Results of capacity retention of the cells comprised with $LiNi_{0.5-x}Mg_xMn_{1.5}O_4$ ($x = 0$, 0.02, 0.05, and 0.1) cathodes cycled at (a) 0.1 and (b) 1C rates at 30 °C.

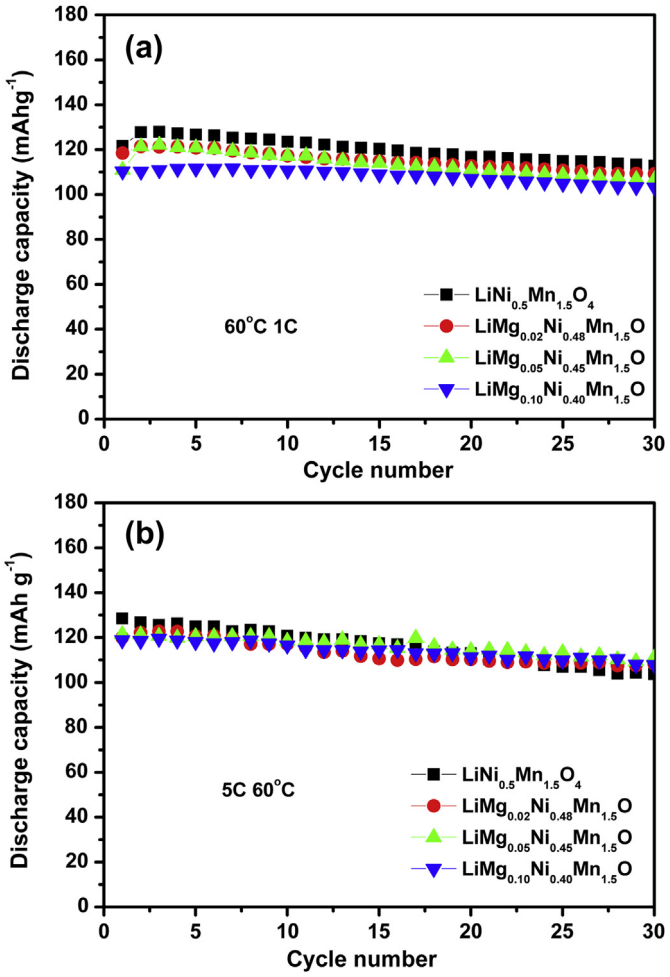

Fig. 10. Results of capacity retention of the cells comprised with $LiNi_{0.5-x}Mg_xMn_{1.5}O_4$ (x = 0, 0.02, 0.05, and 0.1) cathodes cycled at (a) 1 and (b) 5C rates at 60 °C.

deliver similar capacities as those cycled with 1C rate, however, the average capacity fading rates increase significantly (0.71 and 0.52 mAh g^{-1} per cycle for pristine $LiNi_{0.5}Mn_{1.5}O_4$ and $LiNi_{0.4}Mg_{0.1}Mn_{1.5}O_4$, respectively). It manifests that the stabilization effect of Mg-substitution is lowered at elevated temperatures. The reasons are still under investigation.

4. Conclusions

Spinel $LiNi_{0.5-x}Mg_xMn_{1.5}O_4$ (x = 0, 0.02, 0.05, and 0.1) powders were successfully synthesized via spray pyrolysis method. XRD results suggest that Mg-substitution for Ni sites can inhibit the formation of $Li_yNi_{1-y}O$ and increase lattice parameter of the cubic structure. With the aids of Rietveld method, the XRD and NPD results reveal the co-existing of $P4_332$ and $Fd\bar{3}m$ phases in the prepared samples. The fraction of $P4_332$ phase increases with x, indicating the strengthening effect of Mg to the low-temperature phase. The results of capacity retention study recommend that Mg-substitution can suppress the capacity fading of $LiNi_{0.5}Mn_{1.5}O_4$-based materials, however, the effect is lower at elevated temperatures than that at 30 °C.

Acknowledgments

The study had been financially supported by National Science Council (NSC) of Taiwan through a granted project (NSC-99-2632-E-036-001). The authors thank National Synchrotron Radiation Research Center (NSRRC) of Taiwan for the supporting fund (2012-2-123-1) on the research trip and data collection at Bragg Institute, ANSTO, Australia. The authors are also grateful to Dr. V. Peterson and Dr. N. Sharma of Bragg Institute, ANSTO, Australia for their technical support on high-resolution neutron diffraction data collection.

Appendix A. Supplementary data

Supplementary data related to this article can be found at http://dx.doi.org/10.1016/j.jpowsour.2013.04.083.

References

[1] W.-S. Yoon, K.-Y. Chung, K.-H. Oh, K.-B. Kim, J. Power Sources 119–121 (2003) 706–709.
[2] H.W. Chan, J.G. Duh, S.R. Sheen, J. Power Sources 115 (2003) 110–118.
[3] K. Amine, H. Tukamoto, H. Yasuda, Y. Fujita, J. Electrochem. Soc. 143 (1996) 1607–1613.
[4] K. Amine, H. Tukamoto, H. Yasuda, Y. Fujita, J. Power Sources 68 (1997) 604–608.
[5] Y.M. Todorov, Y. Hideshima, H. Noguchi, M. Yoshio, J. Power Sources 77 (1999) 198–201.
[6] L. Guohua, H. Ikuta, T. Uchida, M. Wakihara, J. Electrochem. Soc. 143 (1996) 178–182.
[7] C.H. Shen, R.S. Liu, R. Gundakaram, J.M. Chen, S.M. Huang, J.S. Chen, C.M. Wang, J. Power Sources 102 (2001) 21–28.
[8] R. Thirunakaran, A. Sivashanmugam, S. Gopukumar, C.W. Dunnill, D.H. Gregory, Mater. Res. Bull. 43 (2008) 2119–2129.
[9] S.-C. Park, Y.-M. Kim, Y.-M. Kang, K.-T. Kim, P.S. Lee, J.-Y. Lee, J. Power Sources 103 (2001) 86–92.
[10] Y.-K. Sun, K.-J. Hong, J. Prakash, J. Electrochem. Soc. 150 (2003) A970–A972.
[11] G.H. Wrodnigg, T.M. Wrodnigg, J.O. Besenhard, M. Winter, Electrochem. Commun. 1 (1999) 148–150.
[12] K.Y. Chung, H.S. Lee, W.-S. Yoon, J. McBreen, X.-Q. Yang, J. Electrochem. Soc. 153 (2006) A774–A780.
[13] S. Mandal, R.M. Rojas, J.M. Amarilla, P. Calle, N.V. Kosova, V.F. Anufrienko, J.M. Rojo, Chem. Mater. 14 (2002) 1598–1605.
[14] Q. Zhong, A. Bonakdarpour, M. Zhang, Y. Gao, J.R. Dahn, J. Electrochem. Soc. 144 (1997) 205–213.
[15] Y.K. Yoon, C.W. Park, H.Y. Ahn, D.H. Kim, Y.S. Lee, J. Kim, J. Phys. Chem. Solids 68 (2007) 780–784.
[16] M.N. Obrovac, Y. Gao, J.R. Dahn, Phys. Rev. B 57 (1998) 5728–5733.
[17] C. Sigala, D. Guyomard, A. Verbaere, Y. Piffard, M. Tournoux, Solid State Ionics 81 (1995) 167–170.
[18] T. Ohzuku, S. Takeda, M. Iwanaga, J. Power Sources 81–82 (1999) 90–94.
[19] X. Ma, B. Kang, G. Ceder, J. Electrochem. Soc. 157 (2010) A925–A931.
[20] J.H. Kim, S.T. Myung, C.S. Yoon, S.G. Kang, Y.K. Sun, Chem. Mater. 16 (2004) 906–914.
[21] M. Kunduraci, G.G. Amatucci, Electrochim. Acta 53 (2008) 4193–4199.
[22] D. Pasero, N. Reeves, V. Pralong, A.R. West, J. Electrochem. Soc. 155 (2008) A282–A291.
[23] K. Ariyoshi, Y. Iwakoshi, N. Nakayama, T. Ohzuku, J. Electrochem. Soc. 151 (2004) A296–A303.
[24] M. Kunduraci, G.G. Amatucci, J. Power Sources 165 (2007) 359–367.
[25] Y. Idemoto, H. Narai, N. Koura, J. Power Sources 119 (2003) 125–129.
[26] M. Kunduraci, G.G. Amatucci, J. Electrochem. Soc. 153 (2006) A1345–A1352.
[27] T.A. Arunkumar, A. Manthiram, Electrochim. Acta 50 (2005) 5568–5572.
[28] S.H. Oh, S.H. Jeon, W.I. Cho, C.S. Kim, B.W. Cho, J. Alloys Compd. 452 (2008) 389–396.
[29] Y. Wei, K.-B. Kim, G. Chen, Electrochim. Acta 51 (2006) 3365–3373.
[30] Y.K. Sun, K.J. Hong, J. Prakash, K. Amine, Electrochem. Commun. 4 (2002) 344–348.
[31] D. Li, A. Ito, K. Kobayakawa, H. Noguchi, Y. Sato, J. Power Sources 161 (2006) 1241–1246.
[32] F.G.B. Ooms, E.M. Kelder, J. Schoonman, M. Wagemaker, F.M. Mulder, Solid State Ionics 152–153 (2002) 143–153.
[33] F.G.B. Ooms, M. Wagemaker, A.A. van Well, F.M. Mulder, E.M. Kelder, J. Schoonman, Phys. A: Mater. Sci. Process. 74 (2002) s1089–s1091.
[34] U. Lafont, C. Locati, W.J.H. Borghols, A. Łasińska, J. Dygas, A.V. Chadwick, E.M. Kelder, J. Power Sources 189 (2009) 179–184.
[35] D.W. Shin, C.A. Bridges, A. Huq, M.P. Paranthaman, A. Manthiram, Chem. Mater. 24 (2012) 3720–3731.
[36] D.W. Shin, A. Manthiram, Electrochem. Commun. 13 (2011) 1213–1216.
[37] T.-F. Yi, J. Shu, Y.-R. Zhu, A.-N. Zhou, R.-S. Zhu, Electrochem. Commun. 11 (2009) 91–94.
[38] R. Singhal, M.S. Tomar, J.G. Burgos, R.S. Katiyar, J. Power Sources 183 (2008) 334–338.

[39] D. Li, A. Ito, K. Kobayakawa, H. Noguchi, Y. Sato, Electrochim. Acta 52 (2007) 1919–1924.
[40] K. Ariyoshi, Y. Maeda, T. Kawai, T. Ohzuku, J. Electrochem. Soc. 158 (2011) A281–A284.
[41] B. Hunter, International Union of Crystallography Commission on Powder Diffraction Newsletter No. 20 (Summer) (1998), http://www.rietica.org.
[42] M. Kunduraci, J.F. Al-Sharab, G.G. Amatucci, Chem. Mater. 18 (2006) 3585–3592.